RSC Publishing PCCP

Supramolecular H-bonded Porous Networks at Surfaces: Exploiting Primary and Secondary Interactions in a Bi-component Melamine-Xanthine System

Journal:	*Physical Chemistry Chemical Physics*
Manuscript ID:	CP-COM-02-2013-050891
Article Type:	Communication
Date Submitted by the Author:	28-Feb-2013

Complete List of Authors:	Ciesielski, Artur; Universite Louis Pasteur, Institut de Science et dIngenierie Supramoleculaires Haar, Sebstien; Universite Louis Pasteur, Institut de Science et dIngenierie Supramoleculaires Paragi, Gabor; Hungarian Academy of Sciences, Supramolecular and Nanostructured Materials Research Group; University of Szeged, Department of Medicinal Chemistry Kupihár, Zoltán; University of Szeged, University of Szeged Kele, Zoltán; University of Szeged, University of Szeged Masiero, Stefano; University of Bologna, Department of Organic Chemistry Fonseca Guerra, Célia; VU University, Theoretical Chemistry Bickelhaupt, Matthias; VU University Amsterdam, Theoretical Chemistry; Radboud University Nijmegen, Institute of Molecules and Materials Spada, Gian Piero; University of Bologna, Department of Organic Chemistry Kovács, Lajos; University of Szeged, Department of Medicinal Chemistry Samori, P. ; University of Strasbourg, ISIS

SCHOLARONE™
Manuscripts

Cite this: DOI: 10.1039/c0xx00000x

www.rsc.org/xxxxxx

COMMUNICATIONS

Supramolecular H-bonded Porous Networks at Surfaces: Exploiting Primary and Secondary Interactions in a Bi-component Melamine-Xanthine System

Artur Ciesielski,[a] Sébastien Haar,[a] Gábor Paragi,[b] Zoltán Kupihár,[c] Zoltán Kele,[c] Stefano Masiero,[d] Célia Fonseca Guerra,[e] F. Matthias Bickelhaupt,[e,f] Gian Piero Spada,[d‡] Lajos Kovács*[c] and Paolo Samorì*[a]

Received (in XXX, XXX) Xth XXXXXXXXX 20XX, Accepted Xth XXXXXXXXX 20XX
DOI: 10.1039/b000000x

The control over the formation of a bi-component porous network was attained by the self-assembly at a solid-liquid interface, by exploiting both primary and secondary non-covalent interactions between melamine and N^3-alkylated xanthine modules.

Hydrogen bonding[1] has been extensively used to direct the self-assembly of suitably designed molecular modules into a variety of supramolecular architectures[2] including one-dimensional (1D) linear non-covalent polymers,[3] two-dimensional (2D) networks[4] and three-dimensional (3D) arrangements.[5] Among the numerous examples of supramolecular arrays on solid surfaces, which have been reported to date,[6] those featuring void spaces, so-called 2D porous networks, are of special importance.[7] The main reason for the growing interest in such periodic architectures, either assembled on metals[8] or graphite,[7, 9] is their great potential for technological applications in nanoengineering and, more generally, in nanotechnology.[10] A distinct advantage of porous networks is their regular spatial arrangement of nanometer-sized cavities with uniform, well-defined shapes that can be used for storage functions or to control reactivities.[11] Engineering the structure and function of 2D porous networks requires control over structural features of precursors, i.e. shape, nature, and position of interacting sites, as well as molecular electronic properties and the overall topology of the material. This strategy, known as crystal engineering, has rapidly developed for 2D systems.[12] The spontaneous organization of molecular building blocks into planar, periodic supramolecular architectures is driven by inter- and intra-molecular forces as well as by interfacial interactions. Hydrogen bonds have always been a focus of attention in supramolecular chemistry with much inspiration being drawn from Nature. Besides the multiplicity of H-bonds, the strength of the interactions holding together the molecular units depends on the nature of the donor/acceptor pairs, like the involved heteroatoms, the secondary attractive/repulsive interactions as well as further non-local (e.g. cooperative) effects.[13]

Scanning tunneling microscopy (STM) is one of the most powerful tools to investigate the structure of molecular assemblies at surfaces under various environmental conditions with a sub-molecular resolution.[14] It is therefore an important method to unveil the self-assembly phenomena and 2D crystal engineering with a high degree of precision. The STM application at the solid–liquid interfaces also allows the study of dynamic processes,[15] making this tool very precious for nanochemistry investigations.

Herein, we exploit self-complementary donor-acceptor-donor (DAD) / acceptor-donor-acceptor (ADA) hydrogen bonding to direct the generation of discrete bi-component supramolecular assemblies, which are capable of further self-associating through weak H-bonds to form 2D porous networks at the solid-liquid interface. In particular, we focus our attention on the H-bonding between 1,3,5-triazine-2,4,6-triamine (melamine, ***M***) and N^3-substituted xanthine[16] derivative, i.e. N^3-octadecylxanthine (***X***), capable of forming $\boldsymbol{MX_3}$ entities as shown in Scheme 1.

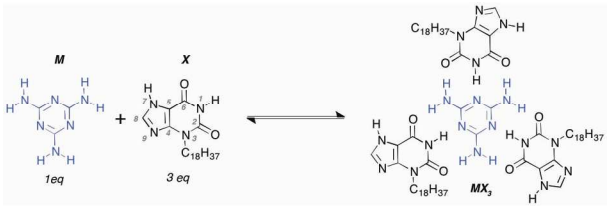

Scheme 1. The molecular structures of investigated molecular modules ***M*** (melamine) and ***X*** (N^3-octadecylxanthine), and the formation of $\boldsymbol{MX_3}$ species through self-complementary H-bonding.

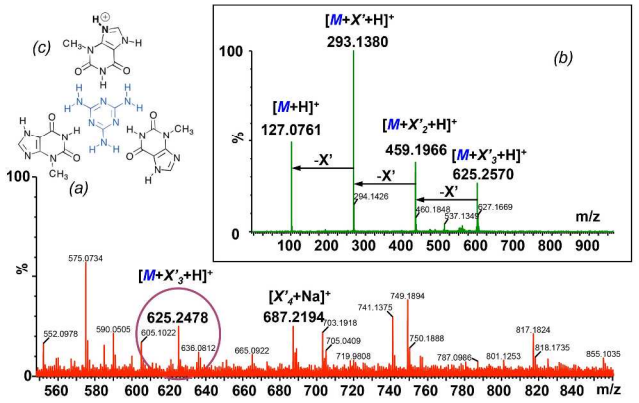

Figure 1. a) ESI-MS spectrum of N^3-methylxanthine (***X'***, MW: 166) and melamine (***M***, MW: 126) in 0.5% aq. formic acid, zoom range *m/z* 550-860; b) CID spectrum of peak at *m/z* 625; c) proposed structure of $[\boldsymbol{MX'_3}+H]^+$ adduct ion.

Because of the very low solubility of N^3-octadecylxanthine (***X***), we have chosen N^3-methylxanthine (***X'***) as a model system in order to study the self-association between xanthine and melamine molecules by electrospray ionization mass spectrometry (ESI-MS).

The ESI-MS spectrum of neat melamine (***M***) in dilute aq. formic acid contained the peaks $[\boldsymbol{M}+H]^+$ and $[\boldsymbol{M_2}+H]^+$ (see Fig. S1 in ESI†). The mass spectrum of neat N^3-methylxanthine contained a series of peaks containing 1-4 xanthine units with proton, sodium or potassium ions (see Fig. S2 in ESI†) with a peak corresponding to the quartet adduct $[\boldsymbol{X'_4}+Na]^+$ at *m/z* 687 being the most abundant as reported.[16a] When the two solutions are mixed together a new adduct appear at *m/z* 625 corresponding to the aggregate $[\boldsymbol{MX'_3}+H]^+$. The intensity (and likely, the stability) of this aggregate was comparable to that of the $[\boldsymbol{X'_4}+Na]^+$ peak at *m/z* 687 (Fig. 1a). This fact suggests that melamine-induced aggregate formation successfully competes with the quartet formation of xanthine, mediated by cations, and efficiently extrudes them to form a stable adduct in which one melamine binds three xanthine molecules by nine H-bonds (Fig. 1c). The identity of the peak $[\boldsymbol{MX'_3}+H]^+$ at *m/z* 625 has been ascertained by tandem mass spectrometric measurements resulting in gradual loss of xanthine molecules to yield adducts $[\boldsymbol{MX'_2}+H]^+$, $[\boldsymbol{MX'}+H]^+$ and finally $[\boldsymbol{M}+H]^+$ (Fig. 1b). As a further evidence of existence of $\boldsymbol{MX_3}$ entities in solution phase ^{1}H NMR analyses of bi-component mixtures have been performed. Modified Job's plot constructed from ^{1}H NMR experiments confirm the existence of a ***X***/***M*** aggregate with 3:1 stoichiometry (see Fig. S6 in ESI†).

STM was used to probe the mono-component self-assembly behavior of ***M*** and ***X***, as well as the bi-component mixture at the solution-graphite interface. STM images of mono-component self-assembled arrays obtained by depositing a drop of solutions of molecular modules ***M*** (12 ± 3 μM) and ***X*** (10 ± 2 μM) in 1,2,4-trichlorobenzene (TCB) on highly oriented pyrolitic graphite (HOPG) surface are displayed in Figure 2a and 2c, respectively. As expected, melamine (***M***) forms a hexagonal pattern (Fig. 2a) with unit cell $a = (0.99 \pm 0.01)$ nm, $b = (1.00 \pm 0.01)$ nm, $\alpha = (62 \pm 2)°$ and $A = (0.89 \pm 0.09)$ nm^2, in very good agreement with that previously observed under UHV conditions[17] and at the solid-liquid interface.[18] The STM height image of the obtained monolayer of N^3-octadecylxanthine (**X**) (Fig. 2c) shows a crystalline structure consisting of ribbon-like architectures. In this 2D crystal, the octadecyl side chains are physisorbed flat on the surface and are interdigitated between adjacent supramolecular ribbons.[19] The unit cell parameters, $a = (1.14 \pm 0.02)$ nm, $b = (2.75 \pm 0.02)$ nm and $\alpha = (83 \pm 2)°$, lead to an area $A = (3.11 \pm 0.03)$ nm^2. The supramolecular packing motif can be described by the formation of the NH(1) – O(2) and NH(7) – O(6) H-bonds between ***X*** modules.

The two aforementioned solutions have been diluted with TCB to yield concentrations of 1 ± 0.1 μM and 3 ± 0.5 μM for ***M*** and ***X***, respectively, and mixed in equal volumes. By applying 4 μL of this new solution to the HOPG surface, a porous network has been obtained at the solid-liquid interface, as visualized by STM imaging at room temperature. Figure 2e shows a 2D hexagonal porous network, which resulted by the formation of: i) strong complementary ***(X)***NH(1) – N***(M)***, ***(X)***O(2) – HN***(M)*** and ***(X)***O(6) – HN***(M)*** H-bonds between ***M*** and ***X***, i.e. the formation of $\boldsymbol{MX_3}$ entities; ii) weak cyclic CH(8) – N(9) H-bonds between ***X*** molecules, i.e. formation of 2D polymeric array. Noteworthy, the octadecyl side chains of ***X*** molecules are backfolded into the supernatant solution, and most likely prevent the growth of assembly in the third dimension, which plays a key role in the formation of porous structure.[20]

To provide molecular understanding of the self-assembly of $\boldsymbol{MX_3}$ species and shed light on the formation and stability of supramolecular $\boldsymbol{(MX_3)_n}$ 2D network, computational studies have been invoked. Taking into account that the observed $\boldsymbol{(MX_3)_n}$ motif was observed only in the presence of a surface, we identified different subsystems which can play an important

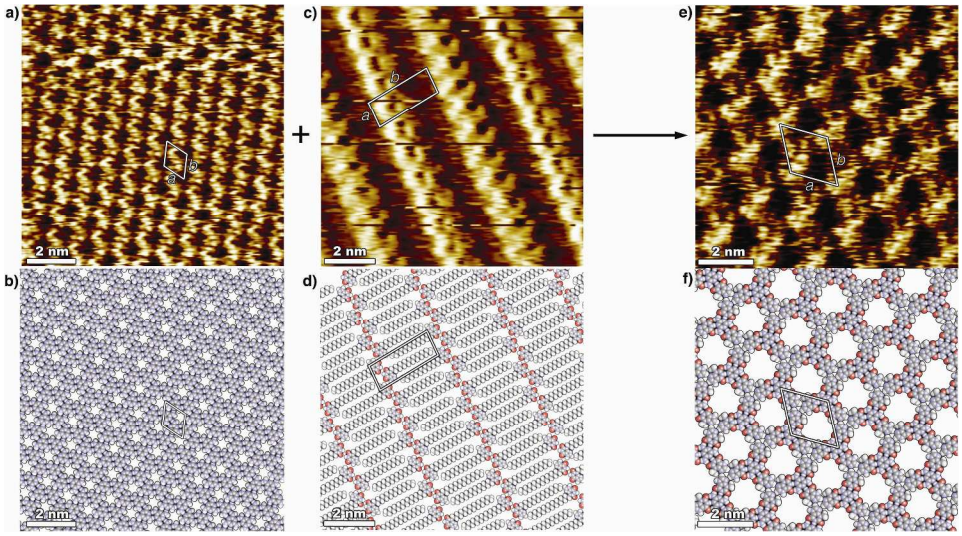

Figure 2. STM height images (*viz.* images recorded in constant current mode) of supramolecular H-bonded structures of: a) melamine (***M***), and c) N^3-octadecylxanthine (***X***) at the 1,2,4-trichlorobenzene-graphite interface. Proposed molecular packing motifs are shown in b) and d), respectively. e) STM height image of the self-assembled $\boldsymbol{(MX_3)_n}$ pattern; f) proposed molecular packing motif of bi-component 2D porous network; for the sake of clarity, octadecyl side chains have been replaced by methyl groups. (a, c and e) Tunneling parameters: average tunneling current $I_t = 25$ - 28 pA, tip bias voltage $V_t = 400 – 450$ mV.

This journal is © The Royal Society of Chemistry [year]

Cite this: DOI: 10.1039/c0xx00000x

www.rsc.org/xxxxxx

role in the formation of the surface-templated 2D pattern. These fragments are shown in Figure 3 (for simplicity the octadecyl side chains have been replaced by methyl groups in the calculations, similarly to the case of MS experiments).

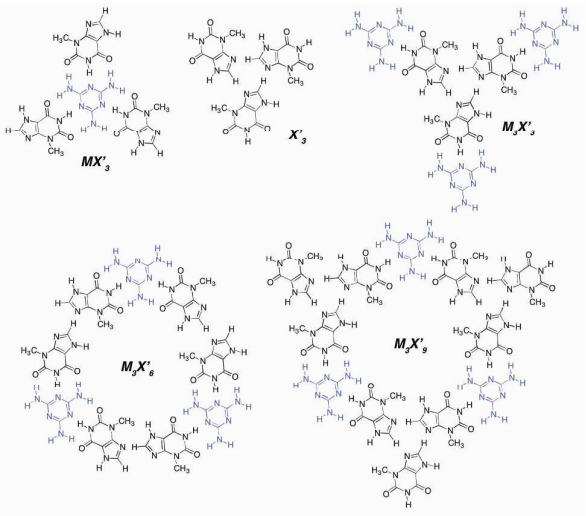

Figure 3. Chemical representation of $(MX'_3)_n$ subunits investigated by density functional theory (DFT) using the BLYP functional (for details see ESI).

Initially, the pre-assembled melamine (***M***) complex with three xanthine (***X'***) molecules (***MX'₃*** in Fig. 3) has been modeled *in silico* at the BLYP-D/TZ2P level of density functional theory. For further computational details see ESI. ***MX'₃*** contains nine strong H-bonds and the crucial question is whether the pyramidal effect on the amino groups of ***M*** can distort the planarity of the complex. Performing optimizations with and without planar constrains, we have found that, albeit the perfectly planar state is a transition state, the unconstrained optimization leads to a nearly planar structure. The total energy difference between the two optima is negligible (less than 0.1 kcal mol^{-1}), highlighting that the ***MX'₃*** entities can easily lay onto a HOPG surface. Comparing corresponding dimer bonding energies (***MX'***, ***X'₂*** or ***M₂*** with values -20.6 kcal mol^{-1}, -16.9 kcal mol^{-1} and -11.8 kcal mol^{-1}, respectively) clearly demonstrates that the interactions between ***M*** and ***X'*** are favorable.

This complex can then easily grow into the ***MX'₃*** species. Consequently, the ***MX'₃*** structure is the most probable complex in the presence of melamine in spite of the fact that the ***X'₄*** quartet has a stronger bonding energy. The bonding energy of the latter structure has been found to be -66.5 kcal mol^{-1} (*cf.* ref.[13b, 16a]) while -58.9 kcal mol^{-1} has been obtained for the ***MX'₃*** complex. Moreover, the ***X'₄*** structure contains only 8 hydrogen bonds therefore the average hydrogen bond is also stronger than in the ***MX'₃*** case. On the other hand, the ***MX'₃*** structure is much more rigid, because of the triple H-bond pattern, therefore it is more likely that the preferred complexation of the melamine-xanthine aggregate is driven by the dimer interaction and the entropic change. Noteworthy, melamine is capable to form a hexameric ring-based structures (see Fig. S9) in the presence of a surface. Nevertheless, this structure is less favorable in the presence of xanthine molecules, because of similar reasons as in the tetrameric case. In addition, the hexameric melamine (***M₆***) ring structure has 12 hydrogen bonds and it reaches its minimum in C_{3i} symmetry. This non-planar geometry is 5.1 kcal mol^{-1} lower in total energy compared to the perfectly planar C_{6h} conformation.

Once ***MX'₃*** species are formed in solution these units can easily lay onto the surface when a graphite support is introduced. As previously hypothesized, the next step towards the formation of 2D bi-component network, has to involve formation of weak intermolecular CH(8) – N(9) H-bonds. Therefore, structures ***X'₃*** and ***M₃X'₃*** were calculated. We found that structure ***X'₃*** is a real minimum in spite of the planar constraint. This system is associated with a bonding energy of -12.4 kcal mol^{-1} with respect to dissociation into three monomers. This bonding energy was not affected by the presence of ***M*** molecules (***M₃X'₃***). We also calculated the interaction energy between one monomer of structure ***X₃*** and the dimer of the remaining two monomers (note that the interaction energy refers to frozen fragments which are not allowed to geometrically relax after dissociation). According to this fragmentation, -9.0 kcal mol^{-1} has been obtained for the interaction energy. Considering the optimized form of structure ***M₃X'₉***, a similar interaction was calculated when dissociating the system into a single xanthine molecule (taken from the corresponding position of the ***M₃X'₃*** structure) and the remaining part of the complex. The interaction energy was found to be -9.6 kcal mol^{-1}, which is very close to the result of the 1+2 decomposition in ***M₃X'₃*** structure. These findings indicate that the different environments do not drastically alter the CH(8) – N(9) interaction which allows the new ***MX'₃*** building blocks to connect properly to the surface-templated structure. Taking into account the large flexibility of structure ***M₃X'₃*** and the weak average CH(8) – N(9) bonding energy (-4.1 kcal mol^{-1}), this structure can form only in the presence of a templating graphite surface. All the calculations support a previously suggested two-step process which leads to the formation of bi-molecular 2D porous structures, i.e. i) formation of the ***MX₃*** unit; ii) simultaneous assembly of ***MX₃*** structures on the surface through weak CH(8) – N(9) interactions. Finally, we have also optimized structures ***M₃X'₆*** and ***M₃X'₉*** by applying the optimized substructures in the setup of the starting geometries. Both optimizations yield a similarly distorted structure ***M₃X'₃*** by slightly changing the geometry of the CH(8) – N(9) connection, but the additional three ***X*** monomers can attach to the structure ***M₃X'₆*** with more similar CH(8) – N(9) geometry (cf. ESI) to that of it acquired in the optimum of structure ***M₃X'₃***. Nevertheless, the triple hydrogen bonds between ***M*** and ***X'*** modules were not affected at all.

Conclusions

We described the bottom-up fabrication of 2D bi-component supramolecular arrays composed of melamine and N^3-octadecylxanthine molecules based on the generation of nine strong H-bonds and the formation of $(MX_3)_n$ discrete assemblies, which are further reinforced by additional CH(8) – N(9) weak interactions. Scanning tunneling microscopy studies at the solid-liquid interface revealed the formation of 2D porous structures. The existence of ***MX'₃***/***MX₃*** species in gas and solution phases

has been corroborated by MS and NMR investigations. The unambiguous assignment of molecular modules was possible by using density functional calculations. The possibility of developing of 2D porous and bi-component polymeric arrays at the solid-liquid interface by making use of secondary weak interactions is of general applicability for the fabrication of stable scaffolds and provides an enhanced control over the super-structure, which can lead to improved properties of the supramolecular materials.

Notes and references

[a] *Nanochemistry Laboratory, ISIS & icFRC, Université de Strasbourg & CNRS, 8 allée Gaspard Monge, 67000, Strasbourg, France. E-mail: samori@unistra.fr; Web: http://www.nanochemistry.fr*
[b] *Research Group of Supramolecular and Nanostructured Materials of the Hungarian Academy of Sciences, Dóm tér 8, 6720 Szeged, Hungary.*
[c] *University of Szeged, Department of Medicinal Chemistry, Dóm tér 8, 6720 Szeged, Hungary.* E-mail: kovacs.lajos@med.u-szeged.hu
[d] *Alma Mater Studiorum – Università di Bologna, Dipartimento di Chimica "G. Ciamician" Via San Giacomo 11 – 40126 Bologna, Italy.*
[e] *Department of Theoretical Chemistry and Amsterdam Center for Multiscale Modeling (ACMM), VU University Amsterdam, De Boelelaan 1083, NL-1081 HV Amsterdam, The Netherlands*
[f] *Institute for Molecules and Materials, Radboud University Nijmegen, Heyendaalseweg 135, NL-6525 AJ Nijmegen, The Netherlands*

† Electronic Supplementary Information (ESI) available: [mass spectroscopy, ^{1}H NMR and computational details]. See DOI: 10.1039/b000000x/

‡ This paper is dedicated to the memory of Professor Gian Piero Spada who passed away on February 3, 2013.

Acknowledgments

This work was financially supported by ERC project SUPRAFUNCTION (GA-257305), the International Center for Frontier Research in Chemistry (icFRC), the EC FP7 ICT-Molarnet project (318516), the COST Action MP0802, the HPC-EUROPA2 228398, the European Commission-Capacities Area-Research Infrastructures, OTKA 73672, MIUR (Italy) in the framework of the National Interest Research Program (PRIN 2009, grant 2009N5JH4F), the Netherlands Organization for Scientific Research (NWO-CW), and the National Research School Combination - Catalysis (NRSC-C).

1. a) G. A. Jeffrey, An Introduction to Hydrogen Bonding, Oxford University Press, 1997; b) G. R. Desiraju, Acc. Chem. Res., 2002, 35, 565-573.
2. a) J.-M. Lehn, Proc. Natl. Acad. Sci. U.S.A., 2002, 99, 4763-4768; b) A. Ciferri, Supramolecular polymers, 2nd ed., Taylor & Francis, Boca Raton, FL, 2005.
3. a) T. Gulik-Krzywicki, C. Fouquey and J.-M. Lehn, Proceedings of the National Academy of Sciences, 1993, 90, 163-167; b) S. De Feyter and F. C. De Schryver, Chem. Soc. Rev., 2003, 32, 139-150; c) M. E. Cañas-Ventura, W. Xiao, D. Wasserfallen, K. Müllen, H. Brune, J. V. Barth and R. Fasel, Angew. Chem. Int. Ed, 2007, 46, 1814-1818; d) A. Ciesielski, G. Schaeffer, A. Petitjean, J. M. Lehn and P. Samorì, Angew. Chem. Int. Ed., 2009, 48, 2039-2043; e) A. Ciesielski, S. Lena, S. Masiero, G. P. Spada and P. Samorì, Ang. Chem. Int. Ed., 2010, 49, 1963-1966.
4. a) S. De Feyter, A. Gesquiere, M. Klapper, K. Müllen and F. C. De Schryver, Nano Lett., 2003, 3, 1485-1488; b) M. Lackinger, S. Griessl, W. A. Heckl, M. Hietschold and G. W. Flynn, Langmuir, 2005, 21, 4984-4988; c) K. Tahara, S. Furukawa, H. Uji-I, T. Uchino, T. Ichikawa, J. Zhang, W. Mamdouh, M. Sonoda, F. C. De Schryver, S. De Feyter and Y. Tobe, J. Am. Chem. Soc., 2006, 128, 16613-16625; d) J. M. MacLeod, O. Ivasenko, D. F. Perepichka and F. Rosei, Nanotechnology, 2007, 18, 424031-424040; e) M. O. Blunt, J. C. Russell, M. D. Gimenéz-López, J. P. Garrahan, X. Lin, M. Schröder, N. R. Champness and P. H. Beton, Science, 2008, 322, 1077-1081; f) K. Tahara, S. Okuhata, J. Adisoejoso, S. B. Lei, T. Fujita, S. De Feyter and Y. Tobe, J. Am. Chem. Soc., 2009, 131, 17583-17590; g) A. Duong, M. A. Dubois and J. D. Wuest, Langmuir, 2010, 26, 18089-18096.
5. a) L. Brunsveld, B. J. B. Folmer, E. W. Meijer and R. P. Sijbesma, Chem. Rev., 2001, 101, 4071-4097; b) D. C. Sherrington and K. A. Taskinen, Chem. Soc. Rev., 2001, 30, 83-93; c) T. F. A. Greef and E. W. Meijer, Nature, 2008, 453, 171-173; d) O. Ivasenko and D. F. Perepichka, Chem. Soc. Rev., 2011, 40, 191-206.
6. a) A. Centrone, E. Penzo, M. Sharma, J. W. Myerson, A. M. Jackson, N. Marzari and F. Stellacci, Proc. Nat. Acad. Sci. USA, 2008, 105, 9886-9891; b) A. Ciesielski, C.-A. Palma, M. Bonini and P. Samorì, Adv. Mater., 2010, 22, 3506-3520; c) E. Gomar-Nadal, M. M. S. Abdel-Mottaleb, S. De Feyter, J. Veciana, C. Rovira, D. B. Amabilino and F. C. De Schryver, Chem.Commun., 2003, 906-907; d) A. M. Jackson, J. W. Myerson and F. Stellacci, Nat. Mater., 2004, 3, 330-336; e) S. Lei, J. Puigmarti-Luis, A. Minoia, M. Van der Auweraer, C. Rovira, R. Lazzaroni, D. B. Amabilino and S. De Feyter, Chem. Commun., 2008, 703-705; f) C.-A. Palma, J. Björk, M. Bonini, M. S. Dyer, A. Llanes-Pallas, D. Bonifazi, M. Persson and P. Samorì, J. Am. Chem. Soc., 2009, 131, 13062-13071.
7. T. Kudernac, S. B. Lei, J. A. A. W. Elemans and S. De Feyter, Chem. Soc. Rev., 2009, 38, 402-421.
8. a) J. V. Barth, Annu. Rev. Phys. Chem., 2007, 58, 375-407; b) D. Kühne, F. Klappenberger, R. Decker, U. Schlickum, H. Brune, S. Klyatskaya, M. Ruben and J. V. Barth, J. Am. Chem. Soc., 2009, 131, 3881-3883; c) D. Bonifazi, H. Spillmann, A. Kiebele, M. de Wild, P. Seiler, F. Y. Cheng, H. J. Guntherodt, T. Jung and F. Diederich, Angew. Chem. Int. Ed, 2004, 43, 4759-4763.
9. N. Katsonis, E. Lacaze and B. L. Feringa, J. Mat. Chem., 2008, 18, 2065-2073.
10. J. V. Barth, G. Costantini and K. Kern, Nature, 2005, 437, 671-679.
11. a) L. Piot, D. Bonifazi and P. Samorì, Adv. Funct. Mater., 2007, 17, 3689-3693; b) J. A. A. W. Elemans, S. B. Lei and S. De Feyter, Angew. Chem. Int. Ed, 2009, 48, 7298-7332.
12. a) F. Cicoira, C. Santano and F. Rosei, Top. Curr. Chem., 2008, 285, 203-267; b) S. Furukawa and S. De Feyter, Top. Curr. Chem., 2008, 287, 87-113; c) K. G. Nath, O. Ivasenko, J. M. MacLeod, J. A. Miwa, J. D. Wuest, A. Nanci, D. F. Perepichka and F. Rosei, J. Phys. Chem. C, 2007, 111, 16996-17007; d) D. Bonifazi, S. Mohnani and A. Llanes-Pallas, Chem. Eur. J., 2009, 15, 7004-7025.
13. a) C. Fonseca Guerra, F. M. Bickelhaupt and E. J. Baerends, Chemphyschem, 2004, 5, 481-487; b) C. Fonseca Guerra, H. Zijlstra, G. Paragi and F. M. Bickelhaupt, Chem. Eur. J., 2011, 17, 12612-12622.
14. a) J. A. A. W. Elemans and S. De Feyter, Soft Matter, 2009, 5, 721-735; b) K. E. Plass, A. L. Grzesiak and A. J. Matzger, Acc. Chem. Res., 2007, 40, 287-293; c) M. Surin and P. Samorì, Small, 2007, 3, 190-194.
15. A. Ciesielski and P. Samori, Nanoscale, 2011, 3, 1397-1410.
16. a) J. Szolomájer, G. Paragi, G. Batta, C. Fonseca Guerra, F. M. Bickelhaupt, Z. Kele, P. Pádár, Z. Kupihár and L. Kovács, New J. Chem., 2011, 35, 476-482; b) M. Yu, J. G. Wang, M. Mura, Q. Q. Meng, W. Xu, H. Gersen, E. Laegsgaard, I. Stensgaard, R. E. A. Kelly, J. Kjems, T. R. Linderoth, L. N. Kantorovich and F. Besenbacher, ACS Nano, 2011, 5, 6651-6660.
17. W. Xu, M. D. Dong, H. Gersen, E. Rauls, S. Vazquez-Campos, M. Crego-Calama, D. N. Reinhoudt, I. Stensgaard, E. Laegsgaard, T. R. Linderoth and F. Besenbacher, Small, 2007, 3, 854-858.
18. C.-A. Palma, M. Bonini, A. Llanes-Pallas, T. Breiner, M. Prato, D. Bonifazi and P. Samori, Chem. Commun., 2008, 5289-5291.
19. A. Ciesielski, S. Haar, A. Bényei, G. Paragi, C. F. Guerra, F. M. Bickelhaupt, S. Masiero, J. Szolomájer, P. Samorì, G. P. Spada and L. Kovács, Langmuir, 2013, DOI: 10.1021/la304540b.
20. We perfomed a series of experiments, where N^3-octadecylxanthine (***X***) was replaced by N^3-methylxanthine (***X'***). Interestingly, 2D melamine-xanthine networks were never observed. Only 3D aggregates, which cannot be characterized by the means of STM.

This journal is © The Royal Society of Chemistry [year]

Supplementary Information

Supramolecular H-bonded Porous Networks at Surfaces: Exploiting Primary and Secondary Interactions in a Bi-component Melamine-Xanthine System

Artur Ciesielski,[a] Sébastien Haar,[a] Gábor Paragi,[b] Zoltán Kupihár,[c] Zoltán Kele,[c] Stefano Masiero,[d] Célia Fonseca Guerra,[e] F. Matthias Bickelhaupt,[e,f] Gian Piero Spada,[d‡] Lajos Kovács*[c] and Paolo Samorì*[a]

[a] *Nanochemistry Laboratory, ISIS & icFRC, Université de Strasbourg & CNRS, 8 allée Gaspard Monge, 67000, Strasbourg, France. E-mail: samori@unistra.fr; Web: http://www.nanochemistry.fr*

[b] *Research Group of Supramolecular and Nanostructured Materials of the Hungarian Academy of Sciences, Dóm tér 8, 6720 Szeged, Hungary.*

[c] *University of Szeged, Department of Medicinal Chemistry, Dóm tér 8, 6720 Szeged, Hungary. E-mail: kovacs.lajos@med.u-szeged.hu*

[d] *Alma Mater Studiorum – Università di Bologna, Dipartimento di Chimica "G. Ciamician" Via San Giacomo 11 – 40126 Bologna, Italy.*

[e] *Department of Theoretical Chemistry and Amsterdam Center for Multiscale Modeling (ACMM), VU University Amsterdam, De Boelelaan 1083, NL-1081 HV Amsterdam, The Netherlands*

[f] *Institute for Molecules and Materials, Radboud University Nijmegen, Heyendaalseweg 135, NL-6525 AJ Nijmegen, The Netherlands*

Table of Contents

1. Mass Spectroscopy

N^3-Methylxanthine and melamine analytes were purchased from TCI and Sigma-Aldrich, respectively. N^3-Octadecylxanthine was prepared as described in ref.[1] Saturated solutions were prepared from both analytes in hot water using a bath sonicator for 10 min. The saturated solutions, containing 0.5% formic acid, were measured first separately, then a 50:50 (v/v) mixture of them.

All mass spectrometric measurements were performed on a Waters Q-TOF Premier spectrometer (Waters, Milford, Massachusetts, USA) equipped with a built-in electrospray ion source. A high voltage of ca. 3000 V was used in the ion source. The instrument was scanned in the normal MS mode over the mass range 50-990 with a scan time of 2 s. In case of MS/MS measurements collision energy was set from 5 to 2 eV. Argon was used as collision gas; gas flow was 0.33 mL/min. Injection volume: 5 µL; Injection speed: 200 µL/min. Cone voltage: 32 V. Eluent: acetonitrile - water 1:1 (v/v).

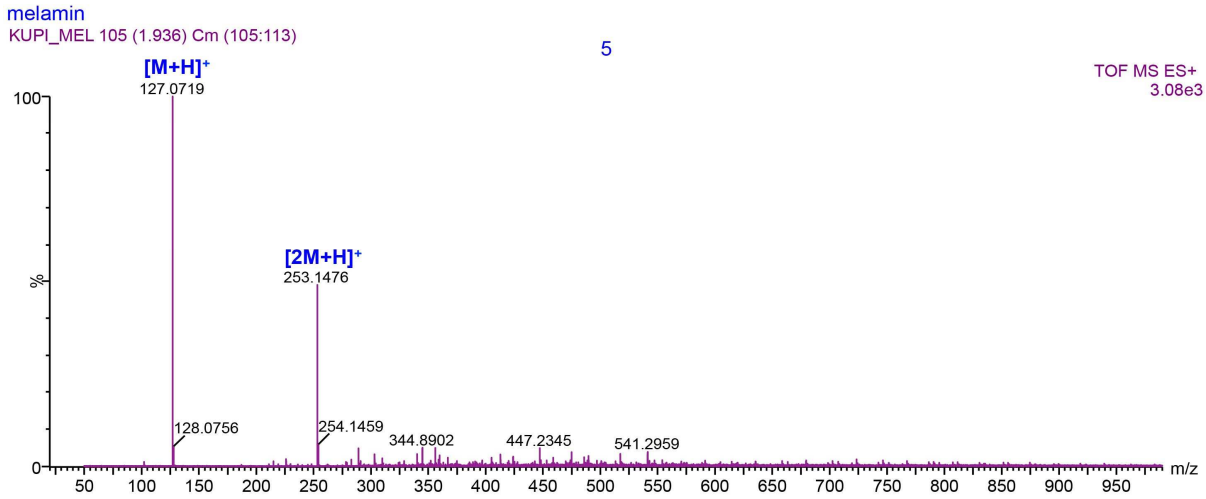

Figure S1. MS spectrum of Melamine (M, MW: 126) in aq. 0.5% formic acid (Q-TOF instrument, positive ion mode).

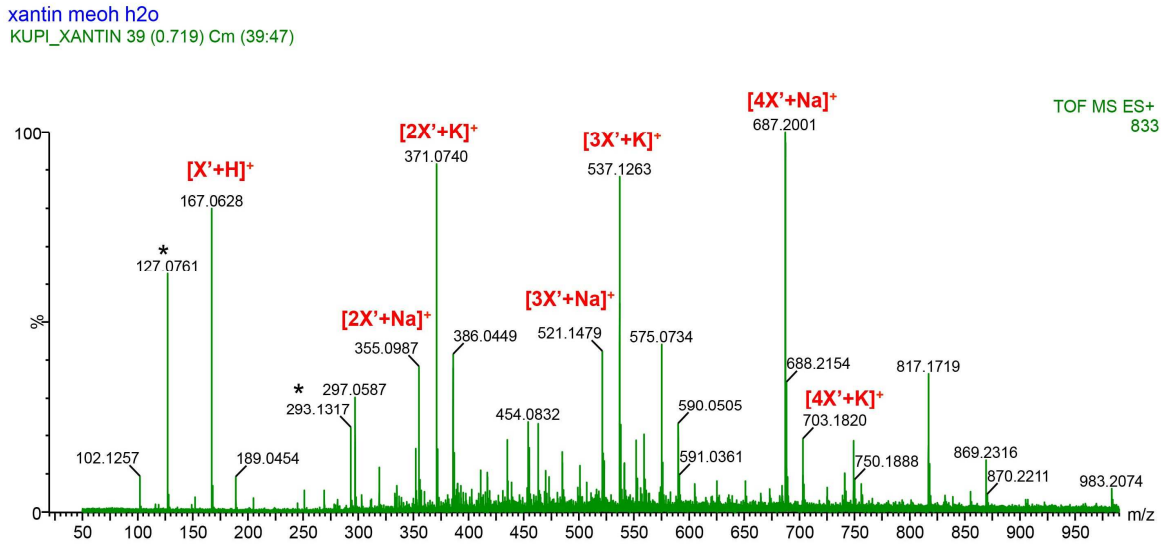

Figure S2. MS spectrum of N^3-Methylxanthine (***X'***, MW: 166) in aq. 0.5% formic acid (Q-TOF instrument, positive ion mode). *Peaks caused by contamination of the needle with melamine.

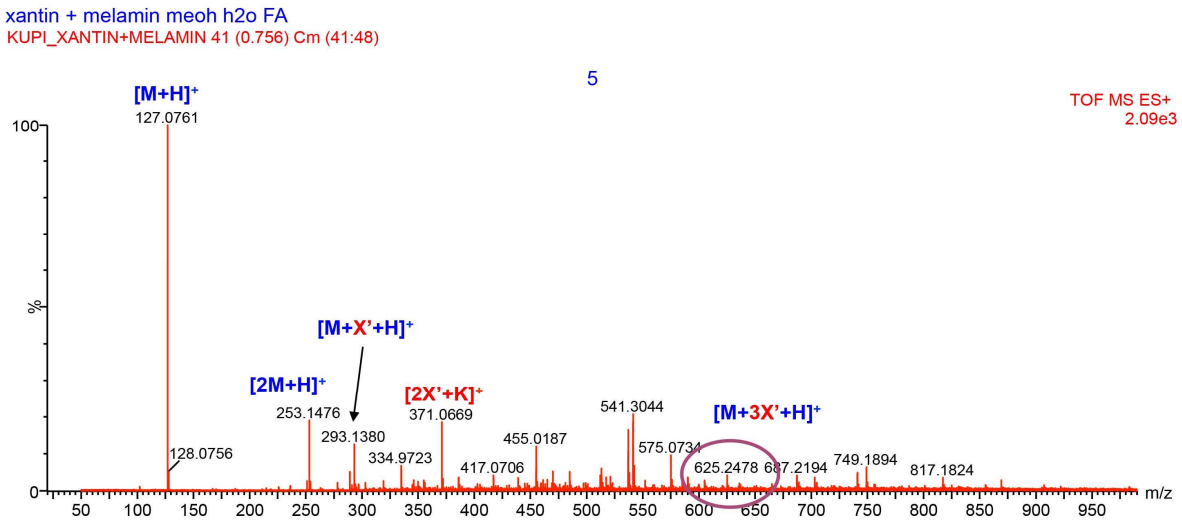

Figure S3. MS spectrum bi-component mixture: N^3-Methylxanthine (***X'***, MW: 166) + Melamine (***M***, MW: 126) in aq. 0.5% formic acid (Q-TOF instrument, positive ion mode).

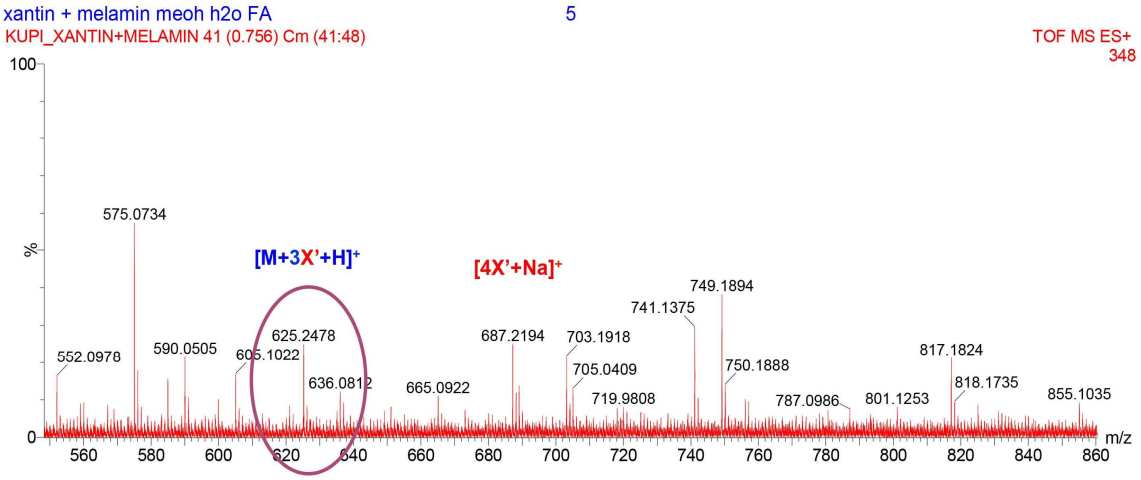

Figure S4. MS spectrum bi-component mixture: N^3-Methylxanthine (***X'***, MW: 166) + Melamine (***M***, MW: 126) in aq. 0.5% formic acid. Zoom range m/z 550 – 860.

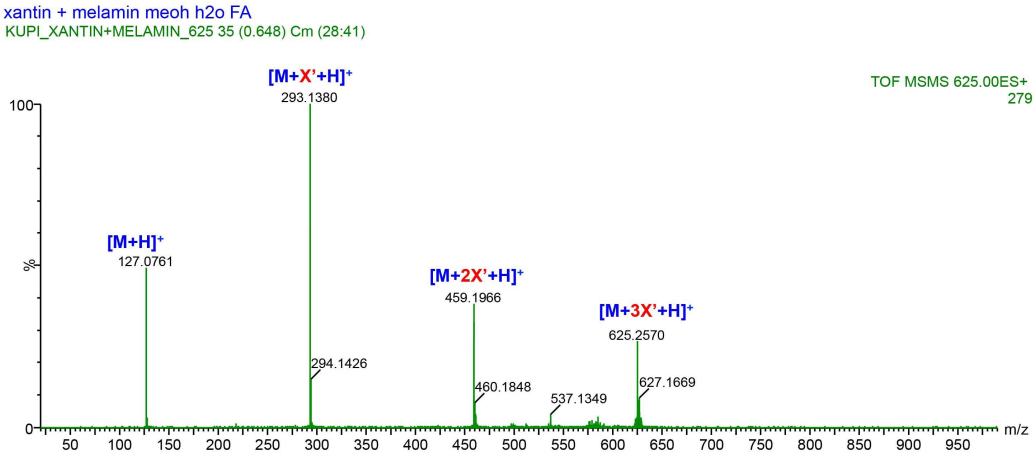

Figure S5. MS spectrum bi-component mixture: N^3-Methylxanthine (***X'***, MW: 166) + Melamine (***M***, MW: 126) in aq. 0.5% formic acid CID spectrum of peak at m/z 625.

2. NMR

NMR spectra were recorded with a Varian Unity INOVA 600 MHz instrument equipped with a reverse probe. Appropriate amounts of ***X*** and ***M*** were weighted and added into NMR tubes. DMSO-d_6 was added to each tube to obtain a 5.3 mM overall composition. Each sample was heated at 353.0 K in the instrument probe and allowed 20 min for dissolution and equilibration before acquiring the spectrum. All measurements were run in duplicate.

Modified Job's plot[2] constructed from ^{1}H NMR experiments, confirm the existence of a ***X***/***M*** aggregate with 3:1 stoichiometry.

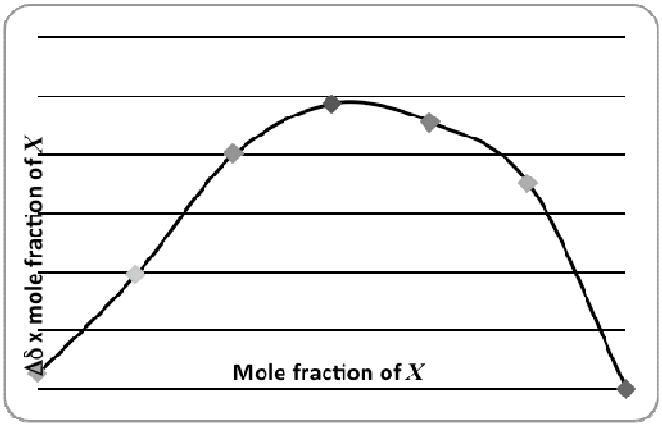

Figure S6. Modified Job's plot [2] of ***X*** and ***M*** (600 MHz, dmso-d_6, 353.0 K). Δδ = chemical shift change of the NH-1 proton of ***X***.[1]

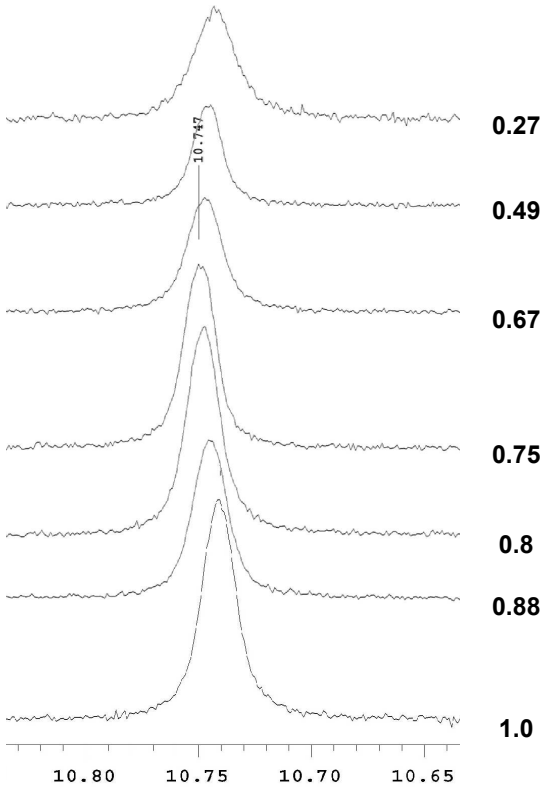

Figure S7. ***X*** NH-1 signal shift in ***X***/***M*** mixtures as a function of ***X*** molar fraction.

3. STM investigation. Scanning Tunneling Microscopy (STM) measurements were performed using a Veeco scanning tunneling microscope (multimode Nanoscope III, Veeco) at the interface between highly oriented pyrolitic graphite (HOPG) and a supernatant solution, by using a scanner A (Veeco), therefore by mapping a maximum area of 1μm × 1μm. Diluted solutions of ***M*** and/or ***X*** were applied to the basal plane of the surface. For STM measurements the substrates were glued on a magnetic disk and an electric contact is made with silver paint (Aldrich Chemicals). The STM tips were mechanically cut from a Pt/Ir wire (90/10, diameter 0.25 mm). The raw STM data were processed through the application of background flattening and the drift was corrected using the underlying graphite lattice as a reference. The latter lattice was visualized by lowering the bias voltage to 20 mV and raising the current to 65 pA. Mother solutions of 1,3,5-triazine-2,4,6-triamine (melamine, ***M***) and N^3-ocadecylxanthine (**X**) were dissolved in 1,2,4-trichlorobenzene (TCB) at 95 ºC and diluted to give 100 μM and 10 μM solutions. STM imaging was carried out in constant current mode yet without turning off the feedback loop, to avoid tip crashes. Monolayer pattern formation was achieved by applying onto freshly cleaved HOPG 4 μL of a solution that was heated at 60-70 ºC to improve the solubility. Noteworthy, study of this system in different solvents, i.e. 1-phenyloctane, nonanoic acid and tetradecane, did not produced any ordered monolayers, which can be attributed to the low solubility of molecules ***M*** and ***X*** in those solvents. The two aforementioned solutions have been diluted with TCB to yield concentrations of 1 ± 0.1 μM and 3 ± 0.5 μM of ***M*** and ***X***, respectively, and mixed in 1:3 (***M***:***X***) ratio. By applying 4 μL of this new solution to the HOPG surface, a porous network has been obtained at the solid-liquid interface, as visualized by STM imaging at room temperature. The STM images were recorded at room temperature after achieving a negligible thermal drift. All of the molecular models were minimized with Chem3D at the MM2 level and processed with QuteMol visualization software. [3]

4. Computational details

All calculations were performed using the 2012 version of Amsterdam Density Functional (ADF),[4] and the QUantum-regions Interconnected by Local Descriptions (QUILD) program developed by Swart and Bickelhaupt.[5] The applied level of density functional theory (DFT) was BLYP-D in combination with the TZ2P basis set: BLYP-D comprises the BLYP functional[6] with dispersion corrections as proposed by Grimme.[7] This approach has been shown to yield excellent structures and energies for multiply-hydrogen bonded DNA-base oligomers.[8] The other reason for including dispersion corrections in the calculations is that, in this way, the new results can have a direct comparison to our previous 3-methylxanthine quadruplex calculations.[8-9]

Equilibrium structures were optimized using analytical gradient techniques and all energy minima except the two largest (12 and 9 units) ones were verified through vibrational analysis.[10] In those cases where it was necessary the presence of a surface was taken into account by planar restraint. The overall bond energy ΔE_{bond} is made up of two major components [Eq. (1)]:

$$\Delta E_{bond} = \Delta E_{def} + \Delta E_{int} \quad (1)$$

The deformation energy ΔE_{def} is the amount of energy required to deform the individual monomer molecule from its equilibrium structure in the gas phase to the geometry that it acquires in the supramolecular complex. The interaction energy ΔE_{int} corresponds to the energy change when the geometrically deformed molecules are associated to form the optimized structure. ADF does not provide total energies, i.e., energies with respect to all nuclei and electrons separated at infinite distance). Instead, it yields energies with respect to separate fragments where default fragments are spherical spin-restricted individual atoms. Note that energy differences with respect to this atomic

zero level provide exactly the same results as calculations with respect to any other point of reference.

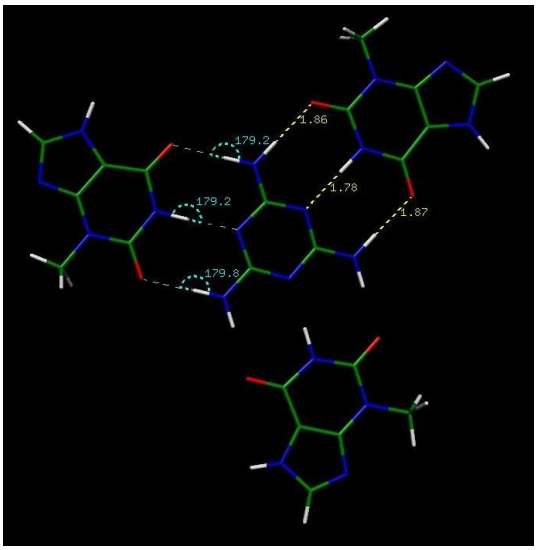

Structure MX'_3

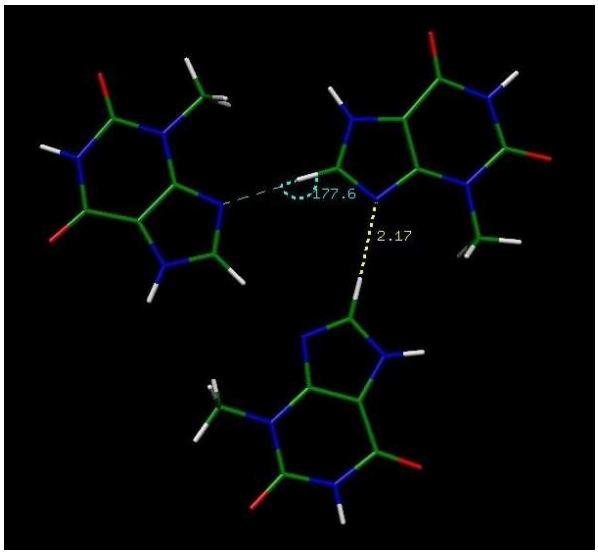

Structure X'_3

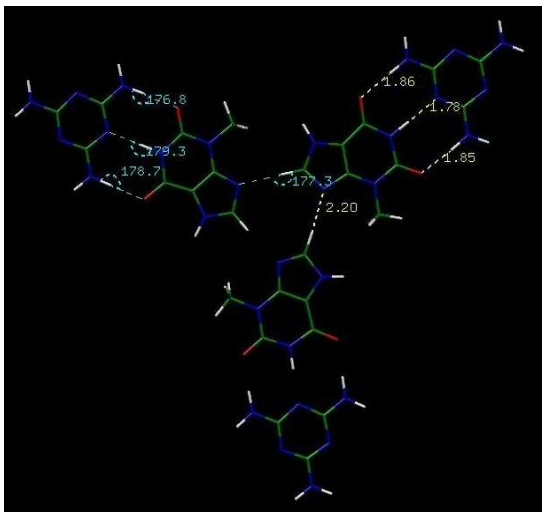

Structure $M_3X'_3$

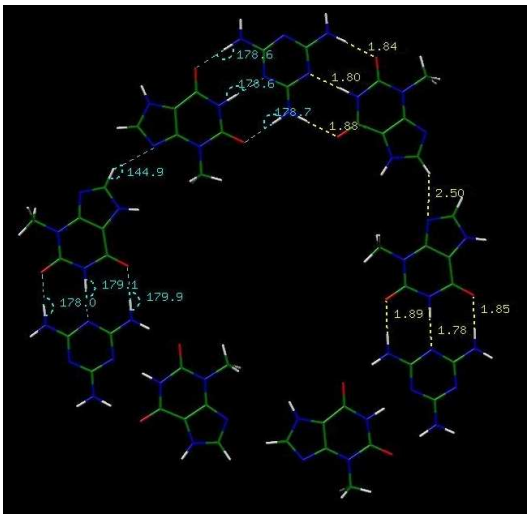

Structure $M_3X'_6$

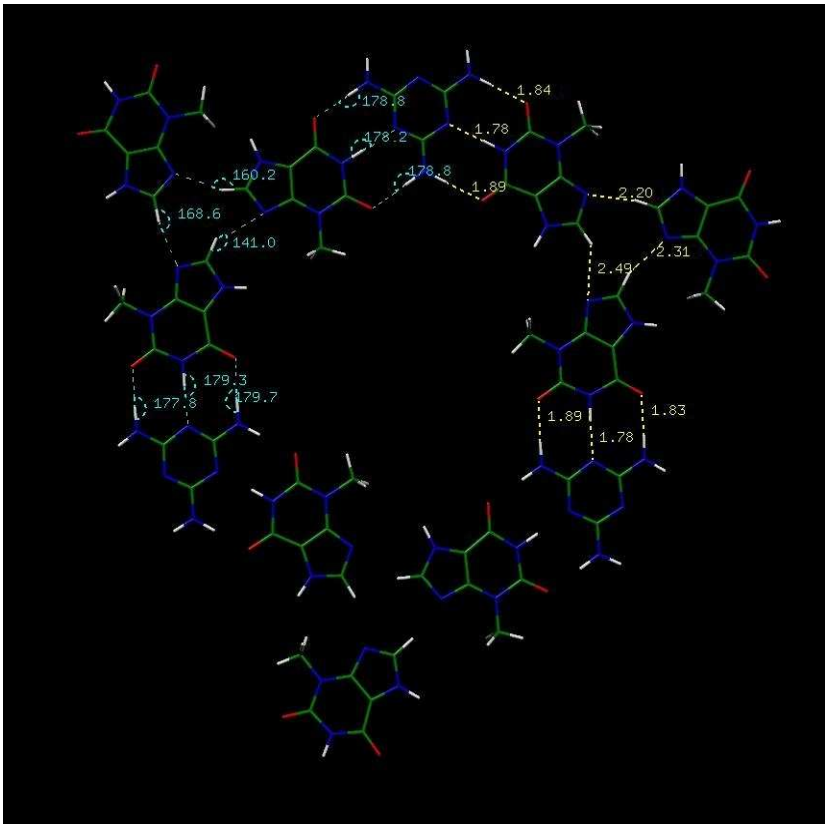

Structure $M_3X'_9$

Figure S8. Optimized H-bond distances (in Å, yellow numbers) and angles (in degree, cyan numbers) of the basic surface motif $M_3X'_9$ and the calculated subsystems (MX'_3, X'_3, $M_3X'_3$, $M_3X'_6$) in the interaction of melamine (***M***) and N^3-methylxanthine (***X'***). All the calculations were performed in C_{3h} symmetry, except structure B where the optimization leads to a non-symmetric structure very close to a C_{3h} symmetric geometry(see main text).

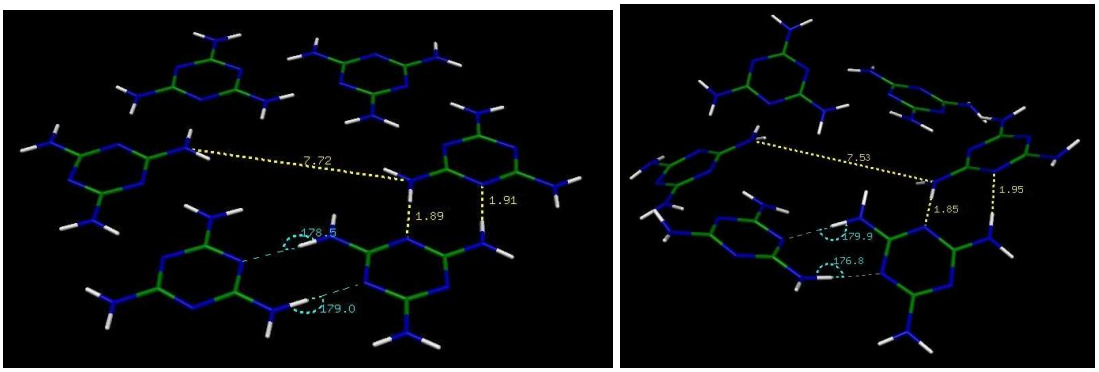

Figure S9. Optimized H-bond distances (in Å, yellow numbers) and angles (in degree, cyan numbers) of hexameric melamine (M_6) in C_{6h} (left) and C_{3i} (right) symmetry.

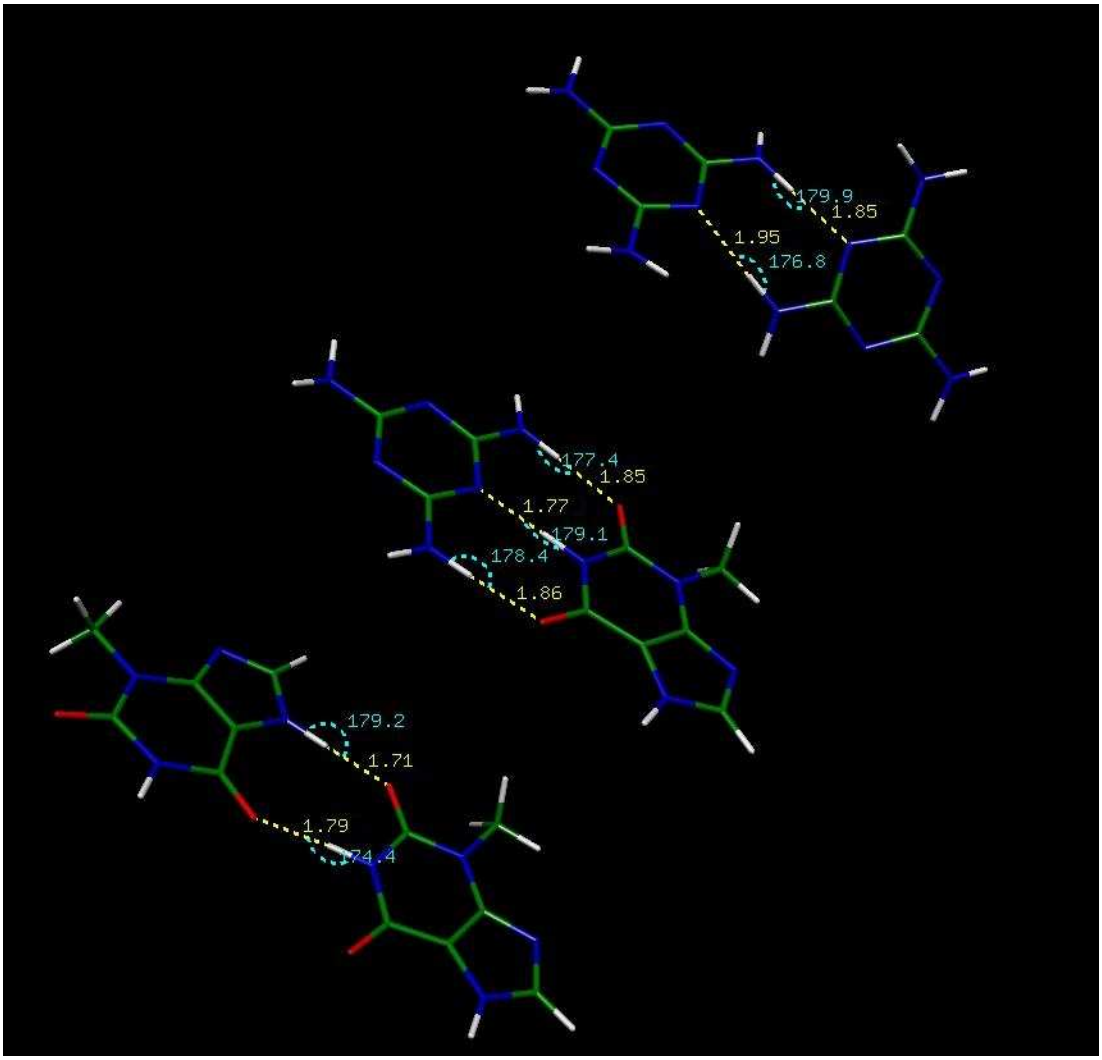

Figure S10. The three optimized reference dimer structures M_2 (top), MX' (middle) and X'_2 (bottom) with optimal H-bond distances (in Å, yellow numbers) and angles (in degree, cyan).

5. References

1. A. Ciesielski, S. Haar, A. Bényei, G. Paragi, C. F. Guerra, F. M. Bickelhaupt, S. Masiero, J. Szolomájer, P. Samorì, G. P. Spada and L. Kovács, *Langmuir*, 2013, DOI: 10.1021/la304540b.
2. K. Hirose, *J. Incl. Phenom. Macrocycl. Chem.*, 2001, **39**, 193-209.
3. M. Tarini, P. Cignoni and C. Montani, *IEEE T. Vis. Comput. Gr.*, 2006, **12**, 1237-1244.
4. a) E. J. Baerends, T. Ziegler, J. Autschbach, D. Bashford, A. Bérces, F. M. Bickelhaupt, P. Bo, P. M. Boerrigter, L. Cavallo, D. P. Chong, L. Deng, R. M. Dickson, D. E. Ellis, M. van Faassen, L. Fan, T. H. Fischer, C. Fonseca Guerra, A. Ghysels, A. Giammona, S. J. A. Van Gisbergen, A. W. Götz, J. A. Groeneveld, O. V. Gritsenko, M. Grüning, S. Gusarov, F. E. Harris, P. van den Hoek, R. Jacob, H. Jacobsen, L. Jensen, J. W. Kaminski, G. van Kessel, F. Kootstra, A. Kovalenko, M. V. Krykunov, E. van Lenthe, D. A. McCormack, A. Michalak, M. Mitoraj, J. Neugebauer, V. P. Nicu, L. Noodleman, V. P. Osinga, S. Patchkovskii, P. H. T. Philipsen, D. Post, C. C. Pye, W. Ravenek, J. I. Rodríguez, P. Ros, P. R. T. Schipper, G. Schreckenbach, J. S. Seldenthuis, M. Seth, J. G. Snijders, M. Sola, M. Swart, D. Swerhone, G. te Velde, P. Vernooijs, L. Versluis, L. Visscher, O. Visser, F. Wang, T. A. Wesolowski, E. M. van Wezenbeek, G. Wiesenekker, S. K. Wolff, T. K. Woo and A. L. Yakovlev,

SCM, ADF2010.01, SCM, Theoretical Chemistry, Vrije Universiteit, Amsterdam, The Netherlands, http://www.scm.com; b) E. J. Baerends, D. E. Ellis and P. Ros, *Chem. Phys.*, 1973, **2**, 41; c) J. G. Snijders, P. Vernooijs and E. J. Baerends, *At. Nucl. Data Tables*, 1981, **26**, 483-509; d) G. te Velde and E. J. Baerends, *J. Comp. Phys.*, 1992, **99**, 84-98; e) C. Fonseca Guerra, O. Visser, J. G. Snijders, G. te Velde and E. J. Baerends, in *Methods and Techniques for Computational Chemistry*, eds. E. Clementi and G. Corongiu, Cagliari, 1995, pp. 305-395; f) C. Fonseca Guerra, J. G. Snijders, G. te Velde and E. J. Baerends, *Theor. Chem. Acc.*, 1998, **99**, 391-403; g) G. te Velde, F. M. Bickelhaupt, E. J. Baerends, C. Fonseca Guerra, S. J. A. Van Gisbergen, J. G. Snijders and T. Ziegler, *J. Comput. Chem.*, 2001, **22**, 931-967.

5. a) M. Swart and F. M. Bickelhaupt, *Int. J. Quantum. Chem.*, 2006, **106**, 2536-2544; b) M. Swart and F. M. Bickelhaupt, *J. Comput. Chem.*, 2008, **29**, 724-734.
6. a) A. D. Becke, *Phys. Rev. A*, 1988, **38**, 3098-3100; b) C. Lee, W. Yang and R. G. Parr, *Phys. Rev. B*, 1988, **37**, 785-789.
7. a) S. Grimme, *J. Comput. Chem.*, 2004, **25**, 1463-1473; b) S. Grimme, *J. Comput. Chem.*, 2006, **27**, 1787-1799.
8. a) C. Fonseca Guerra, T. van der Wijst, J. Poater, M. Swart and F. M. Bickelhaupt, *Theor. Chem. Acc.*, 2010, **125**, 245-252; b) T. van der Wijst, C. Fonseca Guerra, M. Swart, F. M. Bickelhaupt and B. Lippert, *Angew. Chem. Int. Ed.*, 2009, **48**, 3285-3287; c) C. Fonseca Guerra, H. Zijlstra, G. Paragi and F. M. Bickelhaupt, *Chem. Eur. J.*, 2011, **17**, 12612-12622.
9. J. Szolomájer, G. Paragi, G. Batta, C. Fonseca Guerra, F. M. Bickelhaupt, Z. Kele, P. Pádár, Z. Kupihár and L. Kovács, *New J. Chem.*, 2011, **35**, 476-482.
10. a) A. Bérces, R. M. Dickson, L. Y. Fan, H. Jacobsen, D. Swerhone and T. Ziegler, *Comput. Phys. Commun.*, 1997, **100**, 247-262; b) H. Jacobsen, A. Bérces, D. P. Swerhone and T. Ziegler, *Comput. Phys. Commun.*, 1997, **100**, 263-276; c) S. K. Wolff, *Int. J. Quantum. Chem.*, 2005, **104**, 645-659.